

FREEZE THE BACKBONES: A PARAMETER-EFFICIENT CONTRASTIVE APPROACH TO ROBUST MEDICAL VISION-LANGUAGE PRE-TRAINING

Jiuming Qin^{1*}, Che Liu^{2,3*}, Sib0 Cheng^{1,2}, Yike Guo^{2,4}, Rossella Arcucci^{2,3}

¹ Department of Computing, Imperial College London

² Data Science Institute, Imperial College London

³ Department of Earth Science and Engineering, Imperial College London

⁴ Department of Computer Science and Engineering, The Hong Kong University of Science and Technology

ABSTRACT

Modern healthcare often utilises radiographic images alongside textual reports for diagnostics, encouraging the use of Vision-Language Self-Supervised Learning (VL-SSL) with large pre-trained models to learn versatile medical vision representations. However, most existing VL-SSL frameworks are trained end-to-end, which is computation-heavy and can lose vital prior information embedded in pre-trained encoders. To address both issues, we introduce the backbone-agnostic Adaptor framework, which preserves medical knowledge in pre-trained image and text encoders by keeping them frozen, and employs a lightweight Adaptor module for cross-modal learning. Experiments on medical image classification and segmentation tasks across three datasets reveal that our framework delivers competitive performance while cutting trainable parameters by over 90% compared to current pre-training approaches. Notably, when fine-tuned with just 1% of data, Adaptor outperforms several Transformer-based methods trained on full datasets in medical image segmentation.

Index Terms— Vision-Language Pre-training, Self-Supervised Learning, Medical Visual Representation Learning

1. INTRODUCTION

Recent advances in deep learning that combine visual and textual data have achieved significant breakthroughs in the medical field, where available data frequently pairs visual elements, such as radiographs and CT scans, with textual clinical reports [1, 2]. As a result, Vision-Language Self-Supervised Learning (VL-SSL) has emerged as a prevalent pre-training strategy to learn medical representations. It leverages the expansive medical dataset of paired multi-modal data to reduce the dependency on data annotations that traditional supervised training demands [3, 4]. Combined with the rapid developments of domain-specific pre-trained models, researchers can now harness data from multiple modalities

to enhance performance in both uni-modal and multi-modal tasks. Existing works in this field primarily focus on fusing cross-modal information by *aligning* vision and text features with end-to-end training [5, 6, 7, 8]. However, two main challenges arise: (i) the high computational cost and unstable training associated with jointly modelling two distinct modalities with large-sized backbone models [9, 10, 11], and (ii) the risk of diluting prior in-domain information embedded in pre-trained backbones due to finetuning, under-utilising their respective power [12, 13]. Previous studies have assessed the benefits of partially freezing components within vision-language pre-training frameworks, focusing on either language models [14] or vision backbones [13], but not both simultaneously. Recognising that individually freezing sections of language models or vision backbones helps medical image understanding, we investigate the effects of simultaneously freezing both components completely, and present a robust and efficient vision-language pre-training method based on this approach. Our key contributions are as follows:

- We introduce the Adaptor framework with a lightweight, trainable module that effectively integrates knowledge from frozen medical image and text encoders through self-supervised learning. This approach offers notable advantages in parameter efficiency and low computational cost compared to traditional end-to-end pre-training.
- On medical image classification and segmentation tasks over three datasets, Adaptor delivers competitive results while utilising over 90% fewer trainable parameters than current methods. Notably, when fine-tuned on 1% of the data, Adaptor surpasses multiple Transformer-based techniques trained on complete datasets for medical image segmentation.

2. METHODOLOGY

2.1. Problem Definition and Framework

Given a training dataset $\mathcal{D}_{train} = \{(x_i, t_i)\}_{i=1}^N$, consisting of corresponding radiographic images and textual reports, our

* Equal contribution.

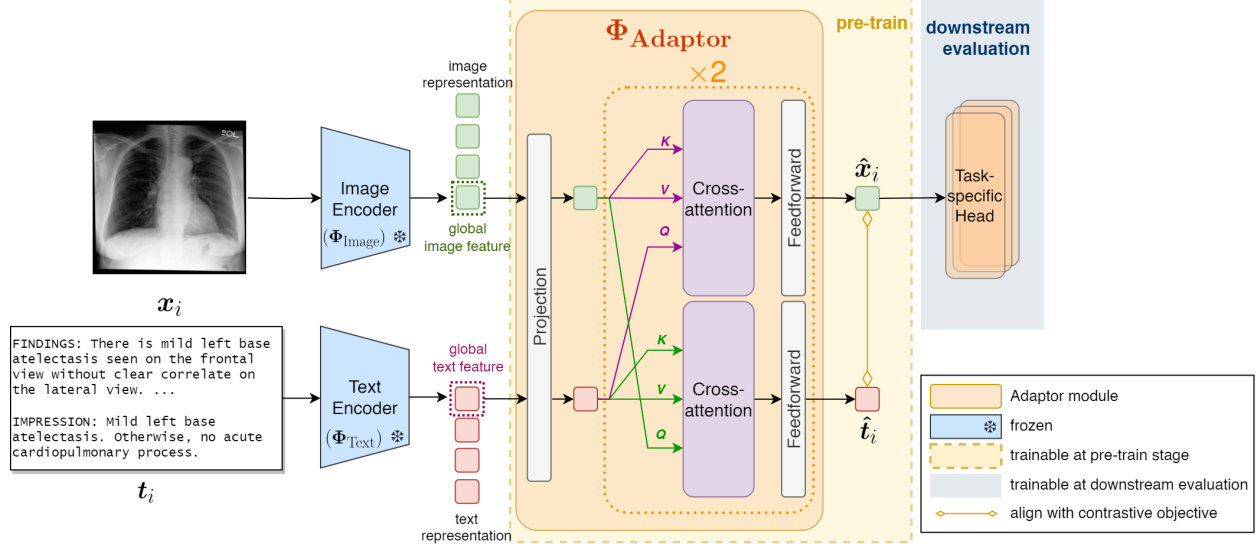


Fig. 1: The Adaptor framework. Note that the duplicated cross-attention and feedforward blocks are identical, only shown this way to demonstrate the different choices of KVQ vectors in the attention mechanism for two modalities. *Blue model blocks* are frozen during both pre-train and finetune, while *yellow and grey blocks* are updated during pre-train and downstream task evaluation stages respectively.

goal is to train a model that jointly processes and understands visual and textual information, resulting in robust medical visual representations. We utilise pre-trained, frozen vision and language backbones to extract uni-modal representations, and introduce an Adaptor module to facilitate cross-modal learning. Figure 1 illustrates our Adaptor framework, which comprises of:

- **Frozen Pre-trained Vision and Language Backbones** ($\Phi_{\text{image}}, \Phi_{\text{text}}$): These transform raw images and texts into individual uni-modal embeddings $\{(\Phi_{\text{image}}(\mathbf{x}_i), \Phi_{\text{text}}(\mathbf{t}_i))\}_{i=1}^N$.
- **Adaptor module** Φ_{Adaptor} : This module projects the vision and text embeddings onto the same dimensionality via a linear layer, then employs two Transformer layers with cross-attention mechanisms to generate multi-modal-aware embeddings, $\hat{\mathbf{x}}_i$ and $\hat{\mathbf{t}}_i$. The resulting image embeddings $\{\hat{\mathbf{x}}_i\}$ are then utilised directly for downstream tasks.

2.2. Pre-training Objective

The pre-training objective jointly models the embeddings of image-text pairs in a shared latent space by minimising a contrastive loss, which enhances the correlation between corresponding image-text pairs and separate the unrelated ones. We sample batches of n image-text pairs, pass them through the frozen dual encoders and the trainable Adaptor module, to obtain multi-modal-aware image embeddings $\hat{\mathcal{X}} = \{\hat{\mathbf{x}}_1, \dots, \hat{\mathbf{x}}_n\}$ and text embeddings $\hat{\mathcal{T}} = \{\hat{\mathbf{t}}_1, \dots, \hat{\mathbf{t}}_n\}$:

$$(\hat{\mathbf{x}}_i, \hat{\mathbf{t}}_j) = \Phi_{\text{Adaptor}}[(\Phi_{\text{image}}(\mathbf{x}_i), \Phi_{\text{text}}(\mathbf{t}_j))], \quad i, j = 1, \dots, n. \quad (1)$$

The image-to-text contrastive loss $\mathcal{L}_{\text{I-T}}$, which takes a similar form as the InfoNCE loss [3], is given by:

$$\mathcal{L}_{\text{I-T}} = -\frac{1}{n} \sum_{k=1}^n \log \frac{\exp\{\langle \hat{\mathbf{x}}_k, \hat{\mathbf{t}}_k \rangle / \tau\}}{\sum_{j=1}^N \exp\{\langle \hat{\mathbf{x}}_k, \hat{\mathbf{t}}_j \rangle / \tau\}}, \quad (2)$$

where $\langle \cdot, \cdot \rangle$ denotes inner product. This loss encourages the model to increase the similarity between the matching image-text pairs $\{(\hat{\mathbf{x}}_k, \hat{\mathbf{t}}_k)\}_{k=1}^n$ and reduce similarities associated with the other text samples in the minibatch. τ is a learnable temperature parameter to further differentiate between positive and negative samples, shown to be effective in enabling the models to learn from hard negatives and proved necessary in vision self-supervised learning [4].

By symmetry, the text-to-image loss, $\mathcal{L}_{\text{T-I}}$, is given by:

$$\mathcal{L}_{\text{T-I}} = -\frac{1}{n} \sum_{k=1}^n \log \frac{\exp\{\langle \hat{\mathbf{x}}_k, \hat{\mathbf{t}}_k \rangle / \tau\}}{\sum_{j=1}^N \exp\{\langle \hat{\mathbf{x}}_j, \hat{\mathbf{t}}_k \rangle / \tau\}}. \quad (3)$$

The final loss \mathcal{L} is a weighted sum of the two:

$$\mathcal{L} = \alpha \mathcal{L}_{\text{I-T}} + (1 - \alpha) \mathcal{L}_{\text{T-I}}, \quad (4)$$

where $\alpha \in (0, 1)$ is a pre-determined weight hyperparameter.

Unlike previous vision-language learning methods that rely the deterministic weight α to introduce asymmetry between textual and visual loss terms [8, 7], our architecture and loss design provide additional flexibility in attending to information from each modality. Specifically, the cross-attention mechanism in the Adaptor module dynamically adjusts the influence of each modality based on training data, offering an implicit, context-aware weighting scheme.

3. EXPERIMENTS

To demonstrate the flexibility and robustness of the Adaptor framework, we evaluated its performance using different combinations among three pre-trained image encoders, namely ResNet autoencoder [15, 16], DINOv2-small and DINOv2-base [17], and five pre-trained language models, which are BERT [18], BioBERT [19], ClinicalBERT [20], CXR-BERT [12] and PubMedBERT [21].

Pre-train. We pre-train the Adaptor framework with the MIMIC Chest X-ray Database v2.0.0 [22], which consists of 277,110 chest radiographs paired with 227,835 medical reports. We adopt the original dataset splits, using the training data for model updates and both validation and test data for model validation. We set the weight hyperparameter α in Equation (4) to be 0.75 as per Zhang et al. [8], and train the model for 50 epochs with a batch size of 1024 and a learning rate of $2e-5$. Since most parameters in the framework remain frozen, we pre-compute and store all output embeddings from frozen encoders in advance, and load them directly as inputs during Adaptor pre-training. This significantly accelerates training, which takes approximately 15 minutes to run on two Tesla T4 GPUs.

Downstream Tasks. We evaluated the framework on two tasks: medical image classification and medical image segmentation. In this stage, both the dual encoders and the pre-trained Adaptor module are kept frozen, as shown in Figure 1. Experiments were conducted on 1%, 10% and 100% of the available labelled data. **Medical image classification:** We use the RSNA Pneumonia [23] and COVIDx CXR-2 datasets [24]. The text encoder is detached from the framework due to the lack of textual inputs at this stage, and a two-layer linear classification head is added on top of the Adaptor. We optimise the cross entropy loss, and report the test set AUROC score for RSNA and accuracy for COVIDx dataset. **Medical image segmentation:** The RSNA Pneumonia [23] and SIIM-ACR datasets [25] are used. We again detach the text encoder and add a decoder after the Adaptor module. For the ResNet Autoencoder, we use a U-Net-style decoder [26], while for the DINOv2 Vision Transformer, an upsampling convolutional decoder is chosen due to the lack of layers in the Transformer architecture.

4. ANALYSIS

Backbone Compatibility. The Adaptor module is widely compatible with different image encoder architectures. In addition to Vision Transformers which naturally yield a global feature, convolutional encoders like ResNet are also compatible when using the channel-wise average of the output feature map as the global uni-modal representation. In Table 1, we show the performance of Adaptors using different backbone models, each fine-tuned with sections of the RSNA dataset. The consistent performance across vision models underscores

the robustness of the Adaptor module when integrated with diverse backbone architectures.

Table 1: Classification AUROC score [%] of Adaptor with different vision and language models on RSNA dataset.

data %	ResNet-AE			DINOv2-S			DINOv2-B		
	1%	10%	100%	1%	10%	100%	1%	10%	100%
BERT	77.0	79.0	81.3	81.3	84.8	86.1	82.8	85.3	86.8
BioBERT	76.8	79.1	81.2	82.2	85.1	86.1	84.4	85.6	86.7
ClinicalBERT	76.7	78.9	81.1	81.7	84.9	86.1	82.9	85.3	86.6
PubMedBERT	76.3	79.0	81.1	80.9	84.5	86.0	82.3	85.0	86.5
CXR-BERT	76.9	79.3	81.5	80.8	84.7	86.0	82.3	85.1	86.6

Parameter efficiency. The standout characteristic of our Adaptor framework is its low computational requirement for training. In Table 2, we present parameter counts alongside the performance of various Vision-Language learning methods for classification tasks. Compared with recent medical VL-SSL approaches utilising large multi-modal encoders and trained end-to-end, the Adaptor framework offers competitive results with a reduction of over 90% in trainable parameters. Figure 2 illustrates the correlation between the classification AUROC score and the number of pre-trained parameters for different methods on the RSNA dataset. While there is a roughly linear correlation between the number of trainable parameters and performance metrics for existing models, the Adaptor framework escapes this linear relationship, achieving performance comparable to large contemporary models with a similar size of trainable parameters as shallow baselines. Utilising the full set of training data, Adaptor with DINOv2-base backbone outperforms ConVIRT [8], with just 8.8% of its parameters to update during training. Table 3 contrasts trainable parameters and performance on the segmentation task. Our Vision-Transformer-based Adaptors, which are set up with a decoder similar in size to previous works, considerably surpass competitors performance trained on full datasets. The ResNet-based Adaptor, although paired with a decoder about twice the size due to its use of ResNet-101 architecture instead of ResNet-50, displays even stronger performance in low-data scenario, achieving superior results with only 1% of the data compared to its peers trained on the full dataset.

Cross-modal fusion. The Adaptor module is able to learn multi-modal dependencies from the fusion operations, which transfers to enhanced downstream task performance. Using the unseen test split of the COVIDx dataset, we visualise in Figure 3 the t-SNE representation of vision embeddings before and after Adaptor processing. In both cases, there is only a vision backbone involved, as the text encoder has been detached at this stage. However, pre-trained textual and cross-modal knowledge has been stored in the weights of the Adaptor module from pre-training. While the pre-trained vision backbone itself struggles to clearly distinguish each class, the enhancements of Adaptor make the three clusters almost linearly separable. It is worth noticing that the Adaptor never received training on classification task signals. This is achieved

Table 2: Parameter count and performance of existing Vision-Language learning methods on medical image classification.

Strategy	Method	Parameters (M)	Trainable (M)	RSNA (AUC)			COVIDx (ACC)		
				1%	10%	100%	1%	10%	100%
Baseline (No Transformer)	DSVE [27]	126.7	5.8	49.7	52.1	57.8	-	-	-
	VSE++ [28]	11.3	11.3	49.4	57.2	67.9	-	-	-
No Medical Pre-training	Random Init	25.6	25.6	58.9	69.4	74.1	50.5	60.3	70.0
	ImageNet Init	25.6	25.6	74.9	74.5	76.3	64.8	78.8	86.3
Medical End-to-End Pre-training	GLoRIA-MIMIC [29, 22]	134.2	134.2	86.1	88.0	88.6	67.3	77.8	89.0
	GLoRIA [29]	134.2	134.2	86.1	88.0	88.6	67.3	77.8	89.0
	ConVIRT [8]	138.1	138.1	77.4	80.1	81.3	72.5	82.5	92.0
	MGCA (ResNet-50) [6]	113.6	113.6	88.6	89.1	89.9	72.0	83.5	90.5
	MGCA (ViT-B) [6]	172.7	172.7	89.1	89.9	90.8	74.8	84.8	92.3
Medical Frozen-Backbone Pre-training (Ours)	Adaptor (ViT-B)	208.3	12.2	84.4	85.6	86.8	71.0	87.5	92.3

Table 3: Trainable parameter count and performance on medical image classification. Dice scores [%] on the test set are reported.

Method	Trainable Param. (M)		RSNA			SIIM		
	Pre-train	Decoder	1%	10%	100%	1%	10%	100%
GLoRIA-MIMIC [29]	134.2	9.0	60.3	68.7	68.3	37.4	57.1	64.0
MGCA (ResNet50-UNet) [6]	113.6	9.0	63.0	68.3	69.8	49.7	59.3	64.2
Adaptor (ResNet-PubMedBERT)	12.0	20.1	76.5	74.3	76.2	73.1	73.1	73.1
Adaptor (ViT/B-BERT)	12.2	10.4	55.9	74.1	77.2	51.8	56.8	73.3
Adaptor (ViT/S-BERT)	11.9	10.4	56.0	71.6	78.1	53.1	58.7	73.7

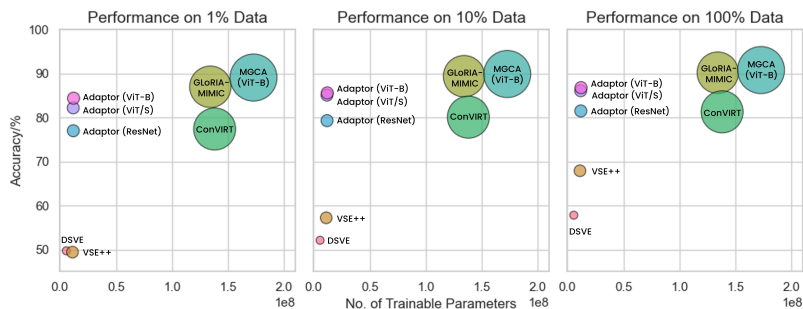


Fig. 2: Number of trainable parameters v.s. performance on RSNA classification. The size of the data points also reflect the number of trainable parameters.

solely by combining the prior information from the text encoder with vision backbone during pre-training, and directly applying this multi-modal knowledge to downstream tasks, showcasing the effectiveness of the fusion.

5. CONCLUSION

We present the Adaptor framework, a parameter-efficient Vision-language Self-Supervised Learning method for enhanced medical vision representation learning. The Adaptor framework freezes pre-trained dual encoders and deploys a backbone-agnostic module with cross-attention for inter-

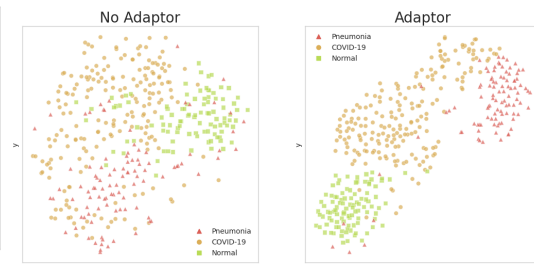


Fig. 3: T-SNE Visualisation of vision embeddings from the COVIDx test dataset, before and after Adaptor module.

modality fusion. This approach is computationally efficient, preserves the depth of medical knowledge from each individual encoder and synergises them to curate enriched, general-purpose medical features. Our method rivals the performance of recent advanced methodologies while maintaining its training requirements at the level of shallow baselines. Empirical evaluations on two medical imaging tasks across three datasets demonstrate the competency of our framework: it achieves competitive results against existing medical vision-language pre-training approaches, while cutting down training costs and reducing tuneable parameters by over 90%.

6. REFERENCES

- [1] Maria Tsimpoukelli, Jacob Menick, Serkan Cabi, S. M. Ali Eslami, Oriol Vinyals, and Felix Hill, “Multimodal few-shot learning with frozen language models,” 2021.
- [2] Alec Radford, Jong Wook Kim, Chris Hallacy, Aditya Ramesh, Gabriel Goh, Sandhini Agarwal, Girish Sastry, Amanda Askell, Pamela Mishkin, Jack Clark, Gretchen Krueger, and Ilya Sutskever, “Learning transferable visual models from natural language supervision,” 2021.
- [3] Aaron van den Oord, Yazhe Li, and Oriol Vinyals, “Representation learning with contrastive predictive coding,” 2019.
- [4] Ting Chen, Simon Kornblith, Mohammad Norouzi, and Geoffrey Hinton, “A simple framework for contrastive learning of visual representations,” 2020.
- [5] Weijie Su, Xizhou Zhu, Yue Cao, Bin Li, Lewei Lu, Furu Wei, and Jifeng Dai, “VL-bert: Pre-training of generic visual-linguistic representations,” 2020.
- [6] Fuying Wang, Yuyin Zhou, Shujun Wang, Varut Vardhanabhuti, and Lequan Yu, “Multi-granularity cross-modal alignment for generalized medical visual representation learning,” *arXiv preprint arXiv:2210.06044*, 2022.
- [7] Philip Müller, Georgios Kaissis, Congyu Zou, and Daniel Rueckert, “Joint learning of localized representations from medical images and reports,” in *Lecture Notes in Computer Science*, pp. 685–701. Springer Nature Switzerland, 2022.
- [8] Yuhao Zhang, Hang Jiang, Yasuhide Miura, Christopher D. Manning, and Curtis P. Langlotz, “Contrastive learning of medical visual representations from paired images and text,” 2022.
- [9] Xiaohua Zhai, Alexander Kolesnikov, Neil Houlsby, and Lucas Beyer, “Scaling vision transformers,” 2022.
- [10] Xinlei Chen, Saining Xie, and Kaiming He, “An empirical study of training self-supervised vision transformers,” 2021.
- [11] Alex Jinpeng Wang, Yixiao Ge, Rui Yan, Yuying Ge, Xudong Lin, Guanyu Cai, Jianping Wu, Ying Shan, Xiaohu Qie, and Mike Zheng Shou, “All in one: Exploring unified video-language pre-training,” 2022.
- [12] Benedikt Boecking, Naoto Usuyama, Shruthi Bannur, Daniel C. Castro, Anton Schwaighofer, Stephanie Hyland, Maria Wetscherek, Tristan Naumann, Aditya Nori, Javier Alvarez-Valle, Hoifung Poon, and Ozan Oktay, “Making the most of text semantics to improve biomedical vision–language processing,” in *Lecture Notes in Computer Science*, pp. 1–21. Springer Nature Switzerland, 2022.
- [13] Ziyuan Qin, Huahui Yi, Qicheng Lao, and Kang Li, “Medical image understanding with pretrained vision language models: A comprehensive study,” 2023.
- [14] Che Liu, Sibao Cheng, Chen Chen, Mengyun Qiao, Weitong Zhang, Anand Shah, Wenjia Bai, and Rossella Arcucci, “M-flag: Medical vision-language pre-training with frozen language models and latent space geometry optimization,” 2023.
- [15] Joseph Paul Cohen, Mohammad Hashir, Rupert Brooks, and Hadrien Bertrand, “On the limits of cross-domain generalization in automated x-ray prediction,” in *Medical Imaging with Deep Learning*, 2020.
- [16] Joseph Paul Cohen, Joseph D. Viviano, Paul Bertin, Paul Morrison, Parsa Torabian, Matteo Guarrera, Matthew P Lungren, Akshay Chaudhari, Rupert Brooks, Mohammad Hashir, and Hadrien Bertrand, “TorchXRyVision: A library of chest X-ray datasets and models,” in *Medical Imaging with Deep Learning*, 2022.
- [17] Maxime Oquab, Timothée Darcet, Theo Moutakanni, Huy V. Vo, Marc Szafraniec, Vasil Khalidov, Pierre Fernandez, Daniel Haziza, Francisco Massa, Alaaeldin El-Nouby, Russell Howes, Po-Yao Huang, Hu Xu, Vasu Sharma, Shang-Wen Li, Wojciech Galuba, Mike Rabbat, Mido Assran, Nicolas Ballas, Gabriel Synnaeve, Ishan Misra, Herve Jegou, Julien Mairal, Patrick Labatut, Armand Joulin, and Piotr Bojanowski, “Dinov2: Learning robust visual features without supervision,” 2023.
- [18] Jacob Devlin, Ming-Wei Chang, Kenton Lee, and Kristina Toutanova, “Bert: Pre-training of deep bidirectional transformers for language understanding,” 2019.
- [19] Jinhyuk Lee, Wonjin Yoon, Sungdong Kim, Donghyeon Kim, Sunkyu Kim, Chan Ho So, and Jaewoo Kang, “BioBERT: a pre-trained biomedical language representation model for biomedical text mining,” *Bioinformatics*, vol. 36, no. 4, pp. 1234–1240, 2020.
- [20] Kexin Huang, Jaan Alntosaar, and Rajesh Ranganath, “ClinicalBERT: Modeling clinical notes and predicting hospital readmission,” 2020.
- [21] Yu Gu, Robert Tinn, Hao Cheng, Michael Lucas, Naoto Usuyama, Xiaodong Liu, Tristan Naumann, Jianfeng Gao, and Hoifung Poon, “Domain-specific language model pretraining for biomedical natural language processing,” 2020.
- [22] Alistair E. W. Johnson, Tom Pollard, Roger Mark, Seth Berkowitz, and Steven Horng, “The mimic-cxr database,” 2019.
- [23] Anouk Stein MD, Carol Wu, Chris Carr, George Shih, Jamie Dulkowski, kalpathy, Leon Chen and Luciano Prevedello, Marc Kohli MD, Mark McDonald, Peter, Phil Culliton, Safwan Halabi MD, and Tian Xia, “RSna pneumonia detection challenge,” 2018.
- [24] Andy Zhao, Hossein, Alexander Wong, Hayden Gunraj, Naomi Waterloo, and May Pal, “Covidx cxr-3,” Jun 2022.
- [25] Jesper, Sören Dramsch, Henrique Mendonça, and Chanran Kim, “Siim acr pneumothorax segmentation data,” Jun 2019.
- [26] Olaf Ronneberger, Philipp Fischer, and Thomas Brox, “U-net: Convolutional networks for biomedical image segmentation,” 2015.
- [27] Martin Engilberge, Louis Chevallier, Patrick Pérez, and Matthieu Cord, “Finding beans in burgers: Deep semantic-visual embedding with localization,” 2018.
- [28] Fartash Faghri, David J. Fleet, Jamie Ryan Kiros, and Sanja Fidler, “Vse++: Improving visual-semantic embeddings with hard negatives,” 2018.
- [29] S. Huang, L. Shen, M. P. Lungren, and S. Yeung, “Gloria: A multimodal global-local representation learning framework for label-efficient medical image recognition,” in *2021 IEEE/CVF International Conference on Computer Vision (ICCV)*, Los Alamitos, CA, USA, oct 2021, pp. 3922–3931, IEEE Computer Society.